Journal Pre-proof

Zone economic model predictive control of a coal-fired boiler-turbine generating system

Yi Zhang, Benjamin Decardi-Nelson, Jianbang Liu, Jiong Shen, Jinfeng Liu

PII: S0263-8762(19)30497-6

DOI: https://doi.org/10.1016/j.cherd.2019.10.027

Reference: CHERD 3862

To appear in: *Chemical Engineering Research and Design*

Received Date: 15 August 2019

Revised Date: 12 October 2019

Accepted Date: 15 October 2019

Please cite this article as: { doi: https://doi.org/

1. An optimal control scheme with zone tracking for coal-fired boiler-turbine systems

2. A detailed economics-oriented control problem formulation and implementation

3. Extensive simulations comparing the proposed design and conventional control

Zone economic model predictive control of a coal-fired boiler-turbine generating system

Yi Zhang[a,b], Benjamin Decardi-Nelson[b], Jianbang Liu[b,c], Jiong Shen[a*], Jinfeng Liu[b*]

[a]Key Laboratory of Energy Thermal Conversion and Control of Ministry of Education, Southeast University, Nanjing 210096, China

[b]Department of Chemical & Materials Engineering, University of Alberta, Edmonton, AB T6G 1H9, Canada

[c]Shenyang Institute of Automation, Chinese Academy of Sciences, Shenyang 110016, China

Abstract

In this work, a zone economic model predictive controller is proposed for the operation of a boiler-turbine generating system. The control objective is to optimize the operating economics while satisfying the power generation demand from the grid. First, the considered boiler-turbine system is introduced and the economic performance indices are formulated. Then, a moving horizon estimator (MHE) is designed to provide state estimates for the controller in virtue of its ability in dealing with nonlinearities and constraints. Subsequently, an economic model predictive control (EMPC) design integrated with a zone tracking objective is proposed for the boiler-turbine generating system. Extensive simulations under different scenarios illustrate the effectiveness of the proposed EMPC design compared with the conventional set-point tracking model predictive control.

*Corresponding authors: J. Shen, Email: shenj@seu.edu.cn; J. Liu, Email: jinfeng@ualberta.ca.

Keywords: Power plant; Moving horizon estimation; Optimal control; Nonlinear systems.

1 Introduction

With more penetration of renewable energy into the electricity supply network, it is necessary for conventional coal-fired power plants to participate in frequency adjustment and peak regulation for the safety and stability of the whole power grid [1]. Due to the randomness and uncertainty in the power generated from renewables, the operation of power plants nowadays is faced with new challenges including frequent and large demand variations. The coordinated control system (CCS) plays a vital role in the stable and economic operation of a power plant, wherein its main responsibility is to drive the boiler-turbine-generator system as one entity and harmonize the slow dynamics of the boiler with the fast dynamics of the turbine and the generator especially during significant load changes [2]. In the operation of a power plant, it is important that the power output meets the demand from the grid while maintaining other important variables like main steam pressure and main steam temperature within their desired ranges [3].

One common control strategy adopted in the control of boiler-turbine systems is the classical proportional-integral-differential (PID) control [4–8]. Different advanced control strategies have also been investigated in the literature, including active disturbance rejection control [9], sliding mode control [10, 11], feedback linearization control [12–14], and model predictive control [15–20]. Among these control strategies, model predictive control (MPC) has become one of the most prevailing techniques in the area of boiler-turbine coordinated control due to its distinct advantages in dealing with multi-input and multi-output systems and constraints. Different MPC algorithms have been investigated including dynamic matrix control [15], multi-model predictive control [16] and nonlinear model predictive control [17], and their variations. In [18], a T-S fuzzy stable model predictive tracking controller is developed for a 600 MW oil-fired drum-type boiler-turbine generating unit to achieve offset-free tracking of the predetermined power and pressure set-points while guaranteeing the input-to-state stability. In [19], a computationally efficient nonlinear model predictive controller is developed by online successively linearizing the local state-space model. In [20], an improved linear extended state observer (ESO) is synthesized with a fuzzy model predictive controller to enhance its disturbance rejection ability by actively estimating and compensating unknown disturbances and model-plant mismatch.

On the other hand, with the increasing worldwide concern of energy shortage and environment conservation, recent researches pay more attention to the economic operation of boiler-turbine systems, such as minimization of fuel consumption and pollution, maximization of system life cycle and economic profits. To achieve economic operation of a boiler-turbine system, the classical two-layer hierarchical control architecture is usually employed [21, 22]. In the architecture, economically optimal steady-states are first calculated through real-time optimization (RTO) in the upper layer [22–24]. The optimal set-points are then transferred to the regulatory controller in the lower layer to track the given set-points. However, it is recognized that this two-layer architecture may lead to sub-optimal or even unreachable set-points [25]. One way to overcome these issues is to integrate the two layers into one single layer wherein a general economic cost is directly optimized at each sampling time. The resulting control scheme is referred to as economic model predictive control (EMPC). Significant efforts have been devoted to the theoretical analysis [26, 27] and application research [28, 29] of EMPC in recent years.

In a boiler-turbine system, the power output set-point, termed as unit load demand, is usually determined by the grid dispatch and the corresponding throttle pressure set-point is obtained from a fixed power-pressure nonlinear mapping [22], which defines the unit's operating policy in the whole power operating range and remains unchanged. The power output and throttle pressure set-points determined through this method cannot take into account the trade-off between different economic objectives, or even unreachable in the presence of significant plant variations or unknown disturbances. In the operation of the boiler-turbine system, the primary task is to satisfy the power demand from the grid in real time while reducing the operational costs. Therefore, the unit load demand tracking requirement should be met first compared with other economic considerations such as the minimization of fuel usage and throttle loss. Motivated by these considerations and inspired by [30–32], an economic MPC with zone tracking design is proposed for boiler-turbine systems in this work. First, the studied 300 MW coal-fired drum-type boiler-turbine system and its model are introduced, and four common performance indices are formulated. Then, a moving horizon estimator (MHE) is employed to provide state estimates for the subsequent controller design due to its distinct ability in dealing with system constraints and nonlinearities. Subsequently, a novel economic MPC with zone tracking design is proposed to optimize the operating economics while satisfying the power generation demand from the grid in real time. To achieve this, a zone tracking cost, which penalizes the distance between power output and the demand target zone, is incorporated into the existing EMPC framework. The conventional two-layer tracking MPC is also introduced for comparison purpose. The simulation results under different scenarios have demonstrated that the proposed EMPC provides a more flexible way to handle the economic optimization problem of the boiler-turbine system in the presence of system nonlinearities, constraints, and disturbances.

The remainder of this paper is organized as follows: a detailed description of the studied 300MW boiler-turbine system along with its sixth-order nonlinear dynamical model and the control problem formulation are presented in Section 2; Section 3 introduces the design of MHE and conventional tracking MPC, and Section 4 provides the design details of the proposed economic MPC with a zone tracking objective. Extensive simulations have been conducted in Section 5 to verify the performance of the proposed EMPC over conventional tracking MPC in load demand tracking, economic performance optimization and disturbance rejection. Finally, some conclusions are drawn in Section 6.

2 System description and performance indices

2.1 System description

In this work, we consider a 300 MW coal-fired drum-type boiler-turbine system as shown in Fig. 1. This system works following a water-steam Rankine cycle. The raw coal in the coal bunker is first transmitted to the mill through the coal feeder and ground into pulverized coal. The pulverized coal is then blew into the boiler furnace and burns there after blended with preheated air. On the steam side, the water flows through the downcomer to the water wall and is heated to saturation condition due to the radiation energy from coal combustion. The saturated steam-water mixer then enters the steam drum, where the steam is separated from the water and flows into the high pressure cylinder after heated by superheater. The exhausted steam of high pressure cylinder is then reheated by reheaters and fed into the middle and low pressure cylinders. The steam turbine is connected to a generator to produce electricity. The exhaust steam discharged from the low pressure cylinder condenses to water in a condenser, which is pumped back to the drum after heated by the economizer and continues the circulation.

Based on mass and energy balances, a sixth-order nonlinear model shown below can de developed

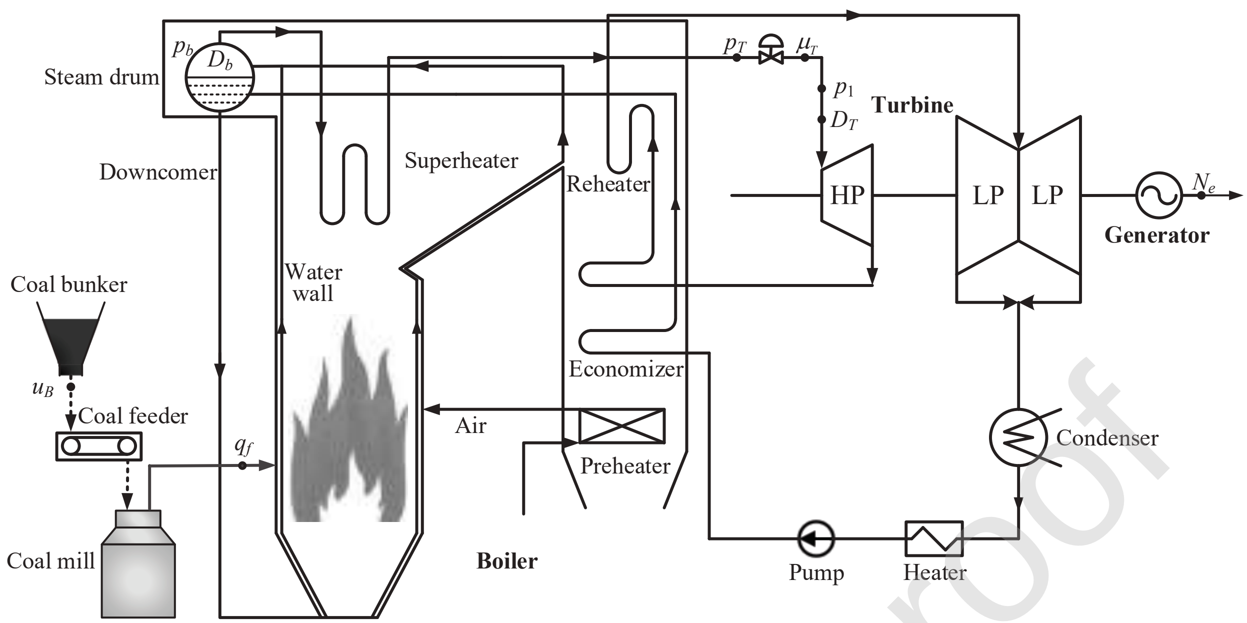

Figure 1: Schematic of the coal-fired drum-type boiler-turbine unit.

103 to describe the dynamics of the above boiler-turbine system [33]:

$$
\begin{aligned}
\dot{q}_f &= \frac{1}{c_1}\left[u_B(t-\tau) - q_f\right] \\
\dot{D}_b &= \frac{1}{c_2}\left(k_1 k_c q_f - D_b\right) \\
\dot{p}_b &= \frac{1}{c_3}\left(D_b - k_2\sqrt{p_b - p_T}\right) \\
\dot{p}_T &= \frac{1}{c_4}\left(k_2\sqrt{p_b - p_T} - D_T\right) \\
\dot{p}_1 &= \frac{1}{c_5}\left(k_3 \mu_T p_T - p_1\right) \\
\dot{D}_T &= \frac{1}{c_6}\left(k_4 p_1 - D_T\right)
\end{aligned}
\tag{1}
$$

where q_f (t/h) is the mass flow rate of the pulverized coal blowing into the furnace, D_b (t/h) is the steam evaporation rate in the drum, p_b (MPa) is the drum pressure, p_T (MPa) is the throttle pressure, p_1 (MPa) is the governing stage pressure, D_T (t/h) is the turbine inlet steam mass flow rate. u_B (t/h) denotes the fuel feed rate and μ_T (%) is the throttle valve opening. τ (s) is the time delay of the coal mill, c_i (s) ($i = 1, \ldots, 6$) are time constants of the coal mill, water wall, drum, superheater, nozzle chamber and reheater, respectively, k_c is the coal heat value coefficient and k_i ($i = 1, \ldots, 5$) are parameters depending on operating conditions.

2.2 Performance indices and control problem formulation

For the boiler-turbine system, two important output variables are the power output N_e (MW) and the throttle pressure p_T (MPa). The power output depends on the turbine inlet steam mass flow rate as $N_e = k_5 D_T$. Two common manipulated inputs are the fuel feed rate u_B and the throttle valve opening μ_T. Let us define the state vector as $x = [\begin{array}{cccccc} q_f & D_b & p_b & p_T & p_1 & D_T \end{array}]^T$, the manipulated input vector as $u = [\begin{array}{cc} u_B & \mu_T \end{array}]^T$, and the process output vector as $y = [\begin{array}{cc} N_e & p_T \end{array}]^T$. Then the boiler-turbine model can be described by a compact nonlinear state-space model as follows:

$$\begin{aligned} \dot{x}(t) &= f(x(t), u_1(t-\tau), u_2(t)) \\ y(t) &= h(x(t)) \end{aligned} \tag{2}$$

The boiler-turbine system is a complex thermodynamic system. A few factors make the optimal operation of this process challenging. First, there is a time delay in the fuel feed as a result of coal grinding process (i.e., the time delay in u_1) which may lead to large pressure variations during load changes. Second, there exists strong coupling between the relatively fast valve-power path and the slower fuel-pressure path. Furthermore, the nonlinearity of the system and the typical wide operating range also intensify operation challenges. Four common performance indices for the operation of the boiler-turbine system are shown below:

$$J_1 = u_1 \tag{3a}$$

$$J_2 = u_2 \tag{3b}$$

$$J_3 = y_1 \tag{3c}$$

$$J_4 = \|y_1 - E_{uld}\|^2 \tag{3d}$$

wherein E_{uld} is unit load demand (MW) from the power grid, J_1 represents the coal consumption, J_2 represents the steam valve opening which is negatively related to the steam valve throttle loss resulting from main steam flowing through the half-open throttle valve, J_3 represents the power output generated by the turbine, and J_4 represents the load tracking error. In order to take into account these four economic performance indices for operation optimization and overcome the aforementioned control difficulties, an economic MPC integrated with a zone tracking objective is proposed for the boiler-turbine system in this work.

3 MHE and conventional tracking MPC

In this section, we introduce MHE and the conventional tracking MPC. We propose to use MHE for state estimation purpose since it can handle nonlinear systems and can take into account constraints [34, 35]. The tracking MPC will be compared with the proposed economic MPC with zone tracking.

3.1 Design of MHE

For the boiler-turbine system, the measured outputs are the power output N_e and the throttle pressure p_T. It can be verified that the entire system state is observable based on these output measurements. In the proposed economic MPC design, the entire system states are needed. This makes the design of a state estimator necessary.

To proceed, we first discretize the continuous-time system (2) and write it in the following form taking into account process and measurement noise:

$$\begin{aligned} x(k+1) &= F(x(k), u_1(k-d), u_2(k)) + w(k) \\ y(k) &= H(x(k)) + v(k) \end{aligned} \tag{4}$$

where $x(k) \in R^6$ is the system state vector at sampling time $t_k = t_0 + k\triangle$ with k being a non-negative integer, t_0 denoting the initial time instant and $\triangle$ being the time interval between two consecutive sampling instants; $y \in R^2$ is the system output vector; function F and H are the corresponding discretized version of f and h in (2), respectively; d is the number of discretization periods in the time delay and is assumed to satisfy $d = \tau/\triangle$; $w \in R^6$ and $v \in R^2$ denote the process disturbance vector and measurement noise vector, respectively. It is assumed that the system inputs (u_1, u_2) are held constant over each sampling period; that is, u_1 and u_2 are piecewise constant functions with a sampling time the same as $\triangle$. It is also assumed that the process disturbance w and measurement noise v are two mutually uncorrelated Gaussian noise sequences and are with zero-mean and covariance matrices Q_w and R_v, respectively.

MHE is an online optimization based approach. At a sampling time, it provides an estimate of the trajectory of the system state within an estimation window by solving a least squares type optimization problem based on the system model and the most recent few measurements and manipulated inputs. It requires that the previous measurements and manipulated inputs are stored. Specifically, at a sampling time t_k, the MHE optimization problem is formulated as follows:

$$\min_{\hat{x}(k-N_m),\{\hat{w}(j)\}_{j=k-N_m}^{k-1}} \quad \sum_{j=k-N_m}^{k-1} \|\hat{w}(j)\|^2_{Q_w^{-1}} + \sum_{j=k-N_m}^{k} \|\hat{v}(j)\|^2_{R_v^{-1}} + \|\hat{x}(k-N_m) - \bar{x}(k-N_m)\|^2_{\Pi^{-1}_{k-N_m}} \tag{5a}$$

$$s.t. \qquad \hat{x}(j+1) = F(\hat{x}(j), u_1(j-d), u_2(j)) + \hat{w}(j) \quad j = k-N_m, ..., k-1 \tag{5b}$$

$$\hat{v}(j) = y(j) - H(\hat{x}_j(j)) \quad j = k-N_m, ..., k \tag{5c}$$

$$\hat{x}(j) \in \mathbb{X} \quad j = k - N_m, ..., k \tag{5d}$$

$$\hat{w}(j) \in \mathbb{W} \quad j = k - N_m, ..., k - 1 \tag{5e}$$

In the above optimization, $\hat{x}$, $\hat{w}$ and $\hat{v}$ represent the estimates of x, w and v, respectively; N_m represents the size of the estimation window. It is assumed that the previous manipulated inputs $(u_1(j-d), u_2)$ $(j = k - N_m, \ldots, k-1)$ and output measurements $y(j)$ $(j = k - N_m, \ldots, k)$ are available within the estimation window. $\mathbb{X}$ and $\mathbb{W}$ denote constraints on system states and disturbances, respectively. The arrival cost term $\|\hat{x}(k-N_m) - \bar{x}(k-N_m)\|^2_{\Pi^{-1}_{k-N_m}}$ summarizes the prior information within the period (t_0, t_{k-N_m}) with Π_{k-N_m} calculated as follows [36]:

$$\Pi_{k+1} = Q_w + A_k \left(\Pi_k - \Pi_k C_k^T (R + C_k \Pi_k C_k^T)^{(-1)} C_k \Pi_k \right) A_k^T \tag{6}$$

where A_k and C_k are the Jacobian matrices at t_k calculated as follows:

$$A_k = \frac{\partial F(x(k), u_1(k-d), u_2(k))}{\partial x(k)^T}, C_k = \frac{\partial H(x(k))}{\partial x(k)^T} \tag{7}$$

In the optimization problem, Eq. (5a) represents the cost function to be minimized with $\hat{x}(k - N_m)$ and $\{\hat{w}(j)\}_{j=k-N_m}^{k-1}$ as the decision variables; Eqs. (5b) and (5c) are system model equations; and Eqs. (5d) and (5e) denote system state and disturbance constraints. At each sampling time t_k, optimal state estimate $\hat{x}^*(k-N_m)$ and process disturbance estimate sequence $\{\hat{w}^*(j)\}_{j=k-N_m}^{k-1}$ can be obtained through solving the optimization problem. Therefore, an estimate of the state trajectory $\hat{x}^*(j)$ $(j = k - N_m, \ldots, k)$ can be calculated based on system model Eq. (5b). Then current state estimate $\hat{x}^*(k)$ is fed to the proposed economic MPC. At next sampling time t_{k+1}, the estimation window is moved forward by one sampling period, and then state estimate $\hat{x}^*(k+1)$ can be obtained.

3.2 Design of tracking MPC

The conventional tracking MPC will be compared with the proposed economic MPC design. For the tracking MPC, the conventional two-layer control structure is used. In the upper RTO layer, a steady-state economic optimization is performed to determine the optimal tracking set-points. The set-points are then sent to the lower layer MPC. In the RTO layer, we consider a weighted summation of the performance indices introduced in Section 2.2 to find the optimal set-points. Specifically, the RTO optimization problem is formulated as follows:

$$\min_{x_s,u_s} \ \alpha_1 J_1 + \alpha_2 J_2 + \alpha_3 J_3 + \alpha_4 J_4 \tag{8a}$$

$$s.t. \ f(x_s, u_{1,s}, u_{2,s}) = 0 \tag{8b}$$

$$u_{min} \leq u_s \leq u_{max} \tag{8c}$$

$$x_{min} \leq x_s \leq x_{max} \tag{8d}$$

wherein α_1, α_2, α_3 and α_4 are the corresponding weights for J_1, J_2, J_3 and J_4, respectively. In this optimization problem, the decision variables are the optimal operating steady-state state and input vectors, Eq. (8a) is the objective function, Eq. (8b) is the steady-state model of the system, Eqs. (8c) and (8d) are the constraints on the system state and input vectors, respectively. By solving this nonlinear optimization problem, the economically optimal operating point (x_s, u_s) can be found for a given unit load E_{uld}, and the corresponding output set-point can be determined based on the output equation and transferred to the lower layer tracking MPC.

In the lower layer, a nonlinear output-feedback tracking MPC controller is designed to track the optimal set-points from RTO layer to improve the load-following capability of the boiler-turbine system. The tracking MPC is formulated as follows:

$$\min_{u(k),u(k+1),\ldots,u(k+N_p-1)} \sum_{i=1}^{N_p} (y(k+i) - y_s(k+i))^T Q\,(y(k+i) - y_s(k+i)) + (u(k+i-1) - u_s(k+i-1))^T R\,(u(k+i-1) - u_s(k+i-1)) \tag{9a}$$

$$s.t. \quad x(k+i) = F(x(k+i-1), u_1(k+i-1-d), u_2(k+i-1)) \quad i = 1, \ldots, N_p \tag{9b}$$

$$y(k+i) = H(x(k+i)) \quad i = 1, \ldots, N_p \tag{9c}$$

$$x(k) = \hat{x}(t_k) \tag{9d}$$

$$u_{min} \le u(k+i-1) \le u_{max} \quad i = 1, \ldots, N_p \tag{9e}$$

$$du_{min} \cdot \triangle \le u(k+i-1) - u(k+i-2) \le du_{max} \cdot \triangle \quad i = 1, \ldots, N_p \tag{9f}$$

$$x_{min} \le x(k+i) \le x_{max} \quad i = 1, \ldots, N_p \tag{9g}$$

where N_p is the prediction horizon, $\triangle$ is the sampling time, $y_s(k+i)$ and $u_s(k+i)$ are the optimal output and input set-points from the RTO layer, Q and R are the weighting matrices on the outputs and control inputs respectively, and $\hat{x}(t_k)$ is the state estimate from MHE at time t_k.

In this optimization problem, Eq. (9a) is the quadratic cost function penalizing the deviations of the system outputs and inputs from the optimal set-points, Eqs. (9b) and (9c) are the model constraints, Eq. (9d) defines the initial condition of the optimization problem at time instant t_k, Eqs. (9e) and (9f) are the physical constraints on the actuator amplitude and increment respectively, and Eq. (9g) is the state constraints for safety reasons. After solving this optimization problem at time t_k, the optimal input sequence $\{u^*(k), u^*(k+1), \cdots, u^*(k+N_p-1)\}$ can be obtained, and the first control input $u^*(k)$ is then applied to the system. At next sampling time t_{k+1}, the MPC is reinitialized with an updated state estimate from the MHE and computes another optimal input sequence.

4 Proposed economic MPC with zone tracking

For the boiler-turbine coordinated control system, the primary task is to track the unit load demand from the grid as close as possible, while keeping the throttle pressure in an acceptable range. Usually, the throttle pressure is set in a set-point calculated from a nonlinear power-pressure mapping or a static multi-objective optimization problem. However, since load condition of a boiler-turbine system changes often, a predetermined set-point at a given load may not be optimal any more, or even unreachable. Moreover, system economics during transient operation have never been considered. In order to take into account the system economic performance during daily operation while always prioritizing load demand tracking, an EMPC with zone tracking is proposed. In the proposed design, a zone tracking cost is incorporated into the EMPC framework to realize unit load demand tracking for improved economic performance. The proposed EMPC optimization problem is formulated as follows:

$$\min_{\substack{u(k),\ldots,u(k+N_p-1)\\ \varepsilon(k+1),\ldots,\varepsilon(k+N_p)}} \sum_{i=1}^{N_p} \|y(k+i)-\varepsilon(k+i)\|_S^2 + (\alpha_1 u_1(k+i-1) + \alpha_2 u_2(k+i-1) + \alpha_3 y_1(k+i)) \tag{10a}$$

$$s.t. \quad x(k+i) = F(x(k+i-1), u_1(k+i-1-d), u_2(k+i-1)) \quad i=1,\ldots,N_p \tag{10b}$$

$$y(k+i) = H(x(k+i)) \quad i=1,\ldots,N_p \tag{10c}$$

$$x(k) = \hat{x}(t_k) \tag{10d}$$

$$u_{min} \leq u(k+i-1) \leq u_{max} \quad i=1,\ldots,N_p \tag{10e}$$

$$du_{min}\cdot\triangle \leq u(k+i-1) - u(k+i-2) \leq du_{max}\cdot\triangle \quad i=1,\ldots,N_p \tag{10f}$$

$$x_{min} \leq x(k+i) \leq x_{max} \quad i=1,\ldots,N_p \tag{10g}$$

$$y_L(k+i) \le \varepsilon(k+i) \le y_H(k+i) \quad i = 1, \ldots, N_p \tag{10h}$$

wherein $\varepsilon(k)$ is the slack variable introduced to realize zone tracking control with weighting matrix S defined as $S = diag([\alpha_4,\ 0])$; $y_L(k)$ and $y_H(k)$ define the lower and upper bound of the target zone for the controlled variables respectively and can be defined as:

$$y_L(k+i) = y_s(k+i) - \delta(k+i) \quad i = 1, \ldots, N_p \tag{11a}$$

$$y_H(k+i) = y_s(k+i) + \delta(k+i) \quad i = 1, \ldots, N_p \tag{11b}$$

wherein $y_s(k)$ corresponds to the original optimal set-points and $\delta(k)$ represents the relaxation value from the original set-points. By setting $\delta(k)$ to zero, the tracking zone of the proposed EMPC will become a set-point line. On the other hand, the set-point tracking objective can be relaxed to a zone tracking objective by setting $\delta(k)$ to a non-zero value. In this way, the output variations within the target zone are ignored, the system is therefore less sensitive to model mismatch and uncertainties, and the overall system becomes more robust.

In this optimization problem, Eq. (10a) is the optimization objective function consisting of both zone tracking cost and economic considerations of the boiler-turbine system, Eqs. (10b) - (10g) are the model constraints, initial state, actuator and state constraints respectively, Eq. (10h) represents the zone constraints of the slack variables. At each sampling time t_k, both the optimal input sequence $\{u^*(k), u^*(k+1), \cdots, u^*(k+N_p-1)\}$ and optimal slack variable sequence $\{\varepsilon^*(k+1), \varepsilon^*(k+2), \cdots, \varepsilon^*(k+N_p)\}$ are calculated simultaneously with the predetermined $\delta(k)$ by solving this optimization problem and the first control input $u^*(k)$ is then applied to the system. At next sampling time t_{k+1}, the proposed EMPC is reinitialized with an updated state estimate from the MHE and computes another optimal input sequence.

Table 1: Model parameters

Static functions	*Dynamic constants*
$k_1 = 2.46q_f^{0.230}$	$\tau = 43$
$k_2 = 42.51p_b^{0.956}$	$c_1 = 22$
$k_3 = 0.0083$	$c_2 = 380$
$k_4 = 74.7$	$c_3 = 4057$
$k_5 = 0.86D_T^{-0.148}$	$c_4 = 5101$
	$c_5 = 5$
	$c_6 = 5$

5 Simulation results

In this section, we apply the proposed EMPC to the boiler-turbine system and compare its performance with the conventional tracking MPC. The optimization problems (MHE, RTO, MPC and EMPC) are solved using IPOPT in Python (version 2.7) based on CasADi (version 3.4.5) - a software framework to facilitate the implementation and solution to optimal control problems using automatic differentiation [37].

5.1 System parameters and constraints

For the boiler-turbine system in Eq. (2), model parameters used in the simulations are given in Table 1. The lower and upper limits of the manipulated inputs are $u_{min} = [\,0\ \ 0\,]^T$ and $u_{max} = [\,150\ \ 100\,]^T$, respectively. The lower and upper limits of the changing rates of the two manipulated inputs are $du_{min} = [\,-0.3\ \ -0.2\,]^T$ and $du_{max} = [\,0.3\ \ 0.2\,]^T$, respectively. The lower and upper limits of system states are $x_{min} = [\,0\ 0\ 0\ 0\ 0\ 0\,]^T$ and $x_{max} = [\,150\ 1200\ 25\ 20\ 20\ 1200\,]^T$, respectively. The lower and upper limits of the two system outputs are $y_{min} = [\,0\ \ 0\,]^T$ and $y_{max} = [\,400\ \ 20\,]^T$, respectively.

5.2 State estimation using MHE

First, the state estimation performance of the MHE scheme introduced in Section 3.1 is illustrated. It is assumed that the two outputs are measured every $\triangle = 5s$ and the measurements are immediately available to the state estimator. We consider that the system is at initially a steady state $x_{s1} = [\,78.9\ 530.1\ 14.9\ 14.0\ 7.1\ 530.1\,]^T$ and the corresponding steady-state input is $u_{s1} = [\,78.9\ 61.2\,]^T$. We consider that the boiler-turbine system is affected by both process disturbance and measurement noise. Specifically, the process disturbance sequence w is generated following normal distribution with zero mean and standard deviation $0.008x_{s1}$ to represent a typical noise condition in actual operations and is bounded between $-0.016x_{s1}$ and $0.016x_{s1}$. Random noise sequence v is Gaussian white noise with zero mean and standard deviation $0.002y_{s1}$ in which y_{s1} is corresponding steady-state output.

The MHE parameters Q_w and R_v are usually chosen as the covariance matrices of the process disturbance w and measurement noise v, respectively. Following this guideline, in this work, $Q_w = diag(\left[(0.008x_{s1}(1))^2, (0.008x_{s1}(2))^2, (0.008x_{s1}(3))^2, (0.008x_{s1}(4))^2,\ (0.008x_{s1}(5))^2,\ (0.008x_{s1}(6))^2\right])$, $R_v = diag(\left[(0.002y_{s1}(1))^2, (0.002y_{s1}(2))^2\right])$. The initial guess of the states in the MHE is $1.2x_{s1}$, and Π_0 represents the confidence in the initial guess and is chosen as $diag([0.2^2\ 0.2^2\ 0.2^2\ 0.2^2\ 0.2^2\ 0.2^2])$. The selection of MHE window length N_m is based on extensive simulations. From simulations, it was found that when N_m is larger than 6, the estimation performance does not improve obviously. Therefore, N_m is chosen to be 6. To illustrate the estimation performance of the MHE, a set of rectangular wave input signals are applied to the nonlinear boiler-turbine system. The resulting trajectories of state estimates given by the MHE and the actual states are shown in Fig. 2. From Fig. 2, it can be seen that the MHE can obtain overall very good state estimates of the boiler-turbine system. Most of the estimates are very close to the actual values except that there exists some relatively larger state estimation errors in the estimates of x_1 and x_2. This is due to the fact

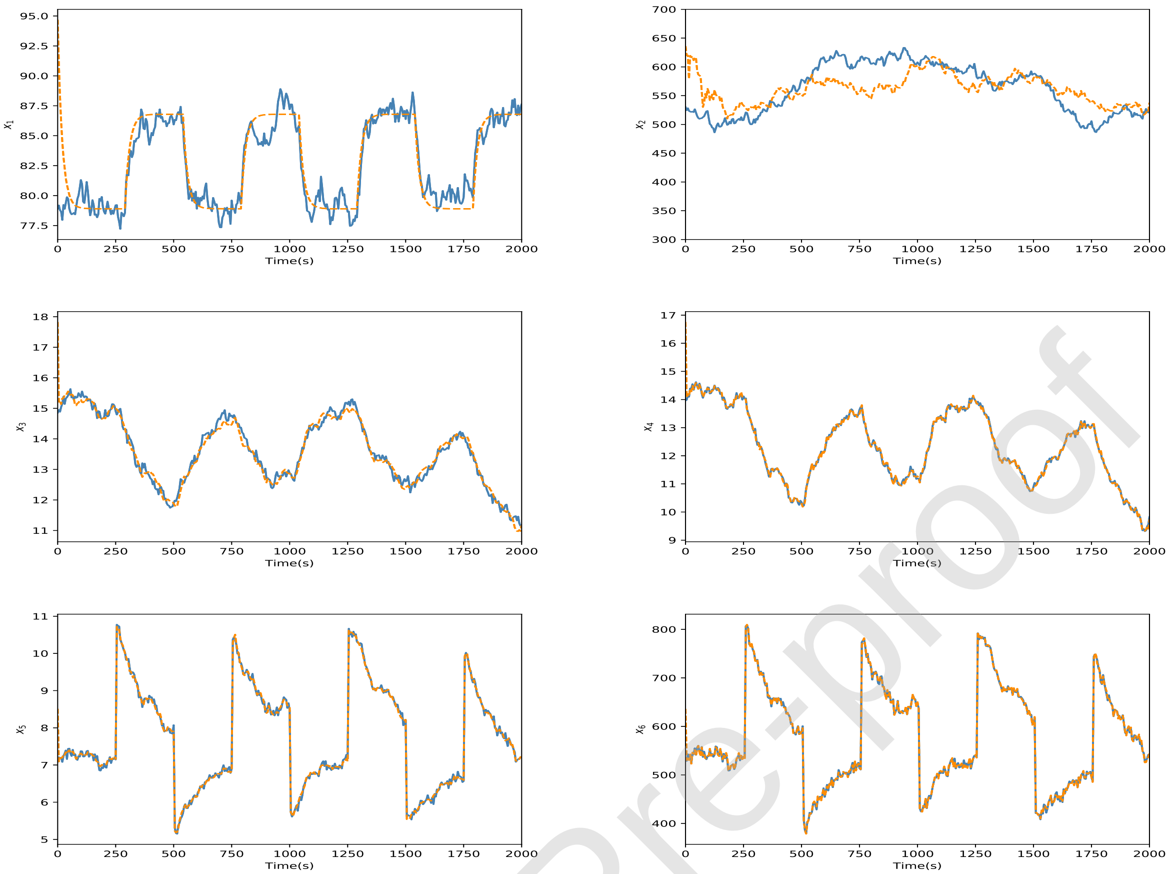

Figure 2: Trajectories of the actual states (blue solid lines) and state estimates by the MHE (orange dashed lines).

that the degree of observability of x_1 and x_2 are relatively lower based on the output measurements of x_4 and x_6. The MHE will be used in combination with the tracking MPC and the economic MPC in Section 5.5.

5.3 Results of load-tracking capability tests

For the boiler-turbine system, generating the required electricity within the required time in response to power grid dispatch is always the top priority. Therefore the load-tracking capability of the proposed EMPC is first verified in this section where fast load demand changes in wide operation range are considered. In this set of simulations, it is assumed that the entire state vector is measured and available to the controllers.

The conventional two-layer tracking MPC is used for comparison. In the optimization problem Eq. (8), α_1 and α_4 are positive while α_2 and α_3 are negative since it is favorable to have reduced coal consumption J_1, small load tracking error J_4 and increased steam valve opening J_2 and increased power output J_3. The values of these weights are selected basically according to the importance of their corresponding terms in the overall objective function. Compared with other weighting parameters, α_4 is chosen to be relatively bigger to ensure that tracking of the given load demand (minimizing the tracking error in J_4) is always given the priority. Therefore, the weighting parameters are chosen as: $\alpha_1 = 0.1$, $\alpha_2 = -0.3$, $\alpha_3 = -0.2$ and $\alpha_4 = 1$. Based on Eq. (8), optimal steady-state reference state and input trajectories according to changing demand are obtained. For the tracking MPC, the sampling time is $\triangle = 5s$, the prediction horizon is $N_p = 120$ to cover most of the dynamics of process. The weighting matrices Q and R represent the importance of output tracking and input tracking respectively. We focus more on tracking the given power output and main steam pressure set-points; therefore, they are chosen as: $Q = diag([200,\ 400])$, $R = diag([1,\ 1])$. For the proposed EMPC, the prediction horizon N_p and sampling time $\triangle$ are chosen to be the same as the tracking MPC, and the weighting parameters α_1, α_2, α_3 are the same as in Eq. (8). The relaxation value $\delta(k)$ in the zone tracking cost is chosen as $[0\ 0]^T$ in this section and its corresponding penalty matrix is chosen as $S = diag([1,\ 0])$ in order to achieve accurate tracking of unit load demand.

Simulations are conducted under two typical cases, of which the first case is to add sequential ramp changes to the unit load demand. Initially, the power output is 210.0 MW and the throttle pressure is 10.2 MPa. At $t = 400s$, the unit load demand begins to decrease from 210.0 MW to 150.0 MW with the load ramping rate of 7.5 MW/min and then begins to increase from 150.0 MW to 180.0 MW at the rate of 3 MW/min at $t = 2400s$. Accordingly, the throttle pressure set-point decreases from 10.2 MPa to 6.9 MPa at $t = 400s$ and then increases from 6.9 MPa to 8.5 MPa at $t = 2400s$. The resulting output variables and control variables of the two control schemes are shown in Fig. 3. It can be seen from Fig. 3 that the power outputs of both the proposed EMPC and the tracking MPC can track the unit load demand closely in both the load decreasing and increasing periods. The inverse response of the throttle pressure of the proposed EMPC and the tracking MPC are basically the same in the load decreasing period except that the EMPC arrives at the output reference trajectory more quickly. However, in the load increasing process, the throttle pressure of EMPC can follow the optimal pressure reference trajectory very tightly while there exists an offset between the throttle pressure of the tracking MPC and the corresponding reference trajectory.

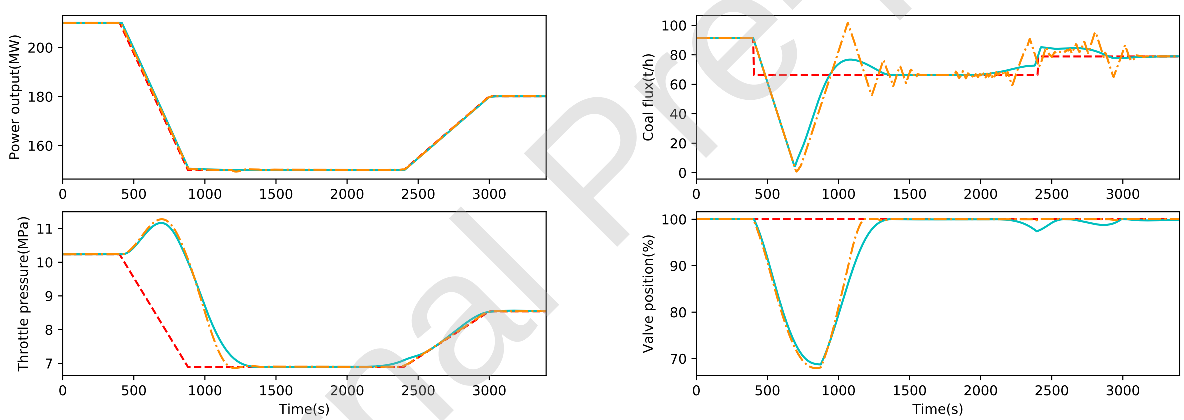

Figure 3: Reference trajectories (red dashed lines), output trajectories (left plot) and input trajectories (right plot) under the EMPC (orange dashed lines) and under the tracking MPC (cyan solid lines) in the presence of ramp changes in the unit load demand.

In the second case, we consider step changes of the unit load demand. Initially, the power output is 210.0 MW and the throttle pressure is 10.2 MPa, then at $t = 400s$ a step change of -30.0 MW is added to the unit load demand, and the throttle pressure set-point decreases from 10.2 MPa to 8.5 MPa accordingly. The resulting output variables and control variables of the two control schemes are shown in Fig. 4. As can be seen from the figures, the power output of EMPC decreases

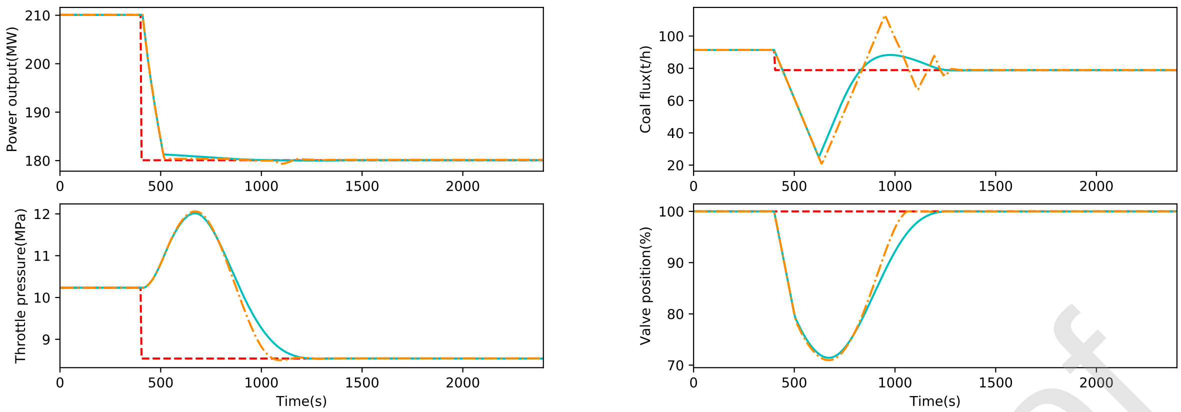

Figure 4: Reference trajectories (red dashed lines), output trajectories (left plot) and input trajectories (right plot) under the EMPC (orange dashed lines) and under the tracking MPC (cyan solid lines) in the presence of step changes in the unit load demand.

to the final steady-state at the maximum speed in response to the sudden decrease in the unit load demand, and the throttle pressure also settles down to the steady-state value more quickly than the tracking MPC. To quantitatively account for the system economic performance, the summation of economic performance index J_{eco} along the simulation time are calculated as follows:

$$E_{eco} = \sum_{i=1}^{N_{sim}} J_{eco}(i) = \sum_{i=1}^{N_{sim}} -(\alpha_1 u_1(i) + \alpha_2 u_2(i)) + \alpha_3 y_1(i)) \tag{12}$$

wherein N_{sim} is the simulation time, J_{eco} (E_{eco}) represents system economic profits and a larger J_{eco} (E_{eco}) value means better economic performance. The resulting performance indexes of the EMPC and the tracking MPC in both cases are summarized in Table 2, and the ratios of E_{eco} of the EMPC to that of the tracking MPC in all cases are also displayed. From this set of simulation, we can see that the proposed EMPC shows similar tracking performance and achieves slight (0.26% to 0.45%) improved economic performance compared with the tracking MPC for load tracking.

Table 2: Economic performance of controllers in the load-following capability tests.

E_{eco}	$400-1600s$ (Case 1)	$1800-3100s$ (Case 1)	$400-1400s$ (Case 2)
EMPC	12753.9 (1.0026)	14113.1 (1.0033)	11142.9 (1.0045)
MPC	12720.4 (1)	14067.2 (1)	11092.8 (1)

5.4 Results of EMPC with different δ values

During the load changing of boiler-turbine systems, unit load demand tracking requirement is not as strict as steady-state condition and tracking errors between the load demand and the actual power output can be maintained within a small range. To take into account this consideration, the set-point tracking of load demand during the transients can be relaxed to a zone tracking objective to obtain more economic performance. This can be realized by setting δ to a non-zero value in Eq. (11), where δ represents the permissible relaxation value from the original set-points. Therefore, different relaxation values δ are tested with the proposed EMPC in this section to verify the economic performance improvement. We consider a ramp decrease in the unit load demand from 210.0 MW to 150.0 MW with the load ramping rate of 7.5 MW/min starting from $t = 400s$, and the throttle pressure set-point decreases from 10.2 MPa to 6.9 MPa accordingly. The proposed EMPC with different relaxation values $\delta = [0\ 0]^T$, $\delta = [3\ 0]^T$, $\delta = [6\ 0]^T$, $\delta = [9\ 0]^T$ are tested. Other simulation parameters of the proposed EMPC and the tracking MPC are the same as in Section 5.3. In this set of simulations, it is also assumed that the entire state measurements are available.

Figure 5 shows the simulation results of the proposed EMPC with different relaxation values during a typical ramp load decrease process. As can be seen from Fig. 5, all of the EMPC controllers can decrease power output to the set-point within the required time while keeping throttle pressure variations in an acceptable range. It is noted that when the first element of δ is not zero, which means the power output is controlled in an predefined operating zone rather than a set-point, the

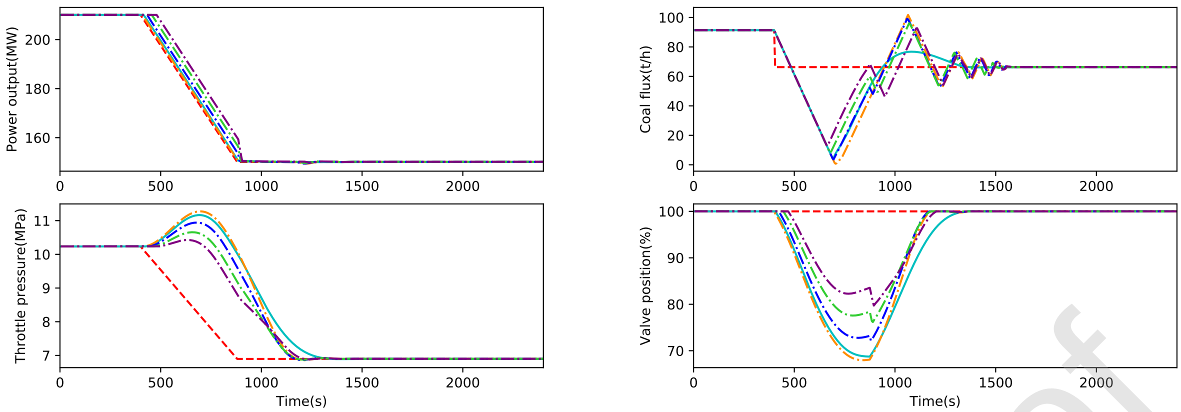

Figure 5: Reference trajectories (red dashed lines), output trajectories (left plot) and input trajectories (left plot) under the proposed EMPC with $\delta = [\,0\;0\,]^T$ (orange dashed lines), $\delta = [\,3\;0\,]^T$(blue dashed lines), $\delta = [\,6\;0\,]^T$(green dashed lines), and $\delta = [\,9\;0\,]^T$ (purple dashed lines), and output trajectories under the tracking MPC (solid cyan lines).

Table 3: E_{eco} of the propsoed EMPC with different δ values

δ	$[0\;\;0]^T$	$[3\;\;0]^T$	$[6\;\;0]^T$	$[9\;\;0]^T$
E_{eco}	15958 (1.0022)	16129.9 (1.0130)	16287.3 (1.0229)	16419.3 (1.0312)

resulting power output is apt to lie in the upper bound of the zone, and the decreasing rate of all the power outputs are the same as the desired ramping rate. Moreover, the throttle pressure under the EMPC with the largest relaxation value δ is the fastest to arrive at new steady-state. Table 3 lists E_{eco} of all the EMPC controllers with different relaxation values during 400-1900s, as well as their ratio to E_{eco} of the tracking MPC (15923.2). It is obvious that the economic performance increases with the increase of the relaxation value δ. The economic performance enhancement reaches up to 3.12% when the relaxation value is chosen as $\delta = [\,9\;0\,]^T$. This is because that when increasing the allowable operating zone of power output during the load changing process, the proposed EMPC gains more degree of freedom to optimize the economics. From this set of simulations, we can see that the proposed EMPC with zone tracking provides a more flexible framework for improved economic performance.

5.5 Results of EMPC subject to coal quality variation

In this section, we consider the effects of a very common disturbance - the variation of coal quality - in the operation of boiler-turbine systems. The variation of coal quality is related to the coal heat value coefficient k_c. First, we evaluate the performance of the proposed EMPC and the tracking MPC subject to the coal quality variation disturbance assuming that the entire state vector is measured. Figures 6 and 7 show the evolution of the system economic cost under the proposed EMPC and the tracking MPC in the case of $k_c = 1.2$ and $k_c = 0.8$, respectively. In Fig. 6, the lower surface represents the steady-state relation between system economic performance index J_{eco} and the two control inputs in the nominal case ($k_c = 1$). In the figure, the red dotted straight line denotes steady states at 80% load, and the red star point (103.77, 100.0, 67.64) at the end of the line denotes the economically optimal steady-state operating point. The upper surface represents the relation between J_{eco} and the two inputs in the steady-state when the k_c value changes to 1.2, in which the blue dotted straight line denotes steady states at 80% unit load, and the blue star point (89.48, 100.0, 69.07) represents the corresponding optimal steady-state operating point.

Here, we consider such a scenario: initially we have a type of coal with $k_c = 1$ and the system is operating at the corresponding optimal steady-state operating point (red star), then due to variation of coal quality, k_c changes to 1.2. Note that this change/disturbance is unknown to the controllers. Note also that this disturbance makes the coal heat efficiency higher and is indeed a favorable disturbance that leads to increased power generation. In such a scenario, the red dotted curve represents the evolution of J_{eco} when the system is controlled by the proposed EMPC, and the blue dotted curve represents the evolution of J_{eco} when the system is controlled by the tracking MPC. Since the coal quality variation is unknown to the controllers, the new optimal operating point (blue star) is unreachable for both of the two controllers. However, since the disturbance is favorable, the proposed EMPC does not try to reject the disturbance as quickly as possible. Instead,

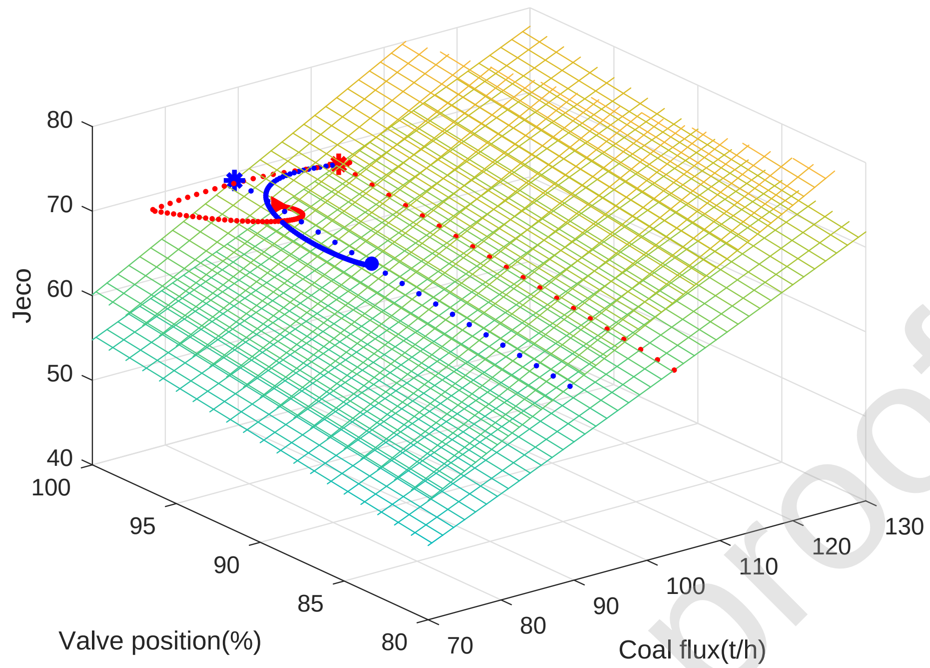

Figure 6: The evolution of economic cost of the system under the proposed EMPC (red dotted line) and the tracking MPC (blue dotted line) in the case of $k_c = 1.2$.

350 the EMPC drives the system state back a new steady-state operating point slowly. However, the
351 tracking MPC still tries to reject the disturbance quickly and keeps the system close to the new
352 steady-state operating point. It is obvious that the proposed EMPC settles at a point (red triangle)
353 that is much closer to the new optimal steady-state operating point than that of the tracking MPC
354 (blue dot), thus better economic performance can be obtained by the propsoed EMPC.

355 When the variation in coal quality makes $k_c = 0.8$, the heat coefficient decreases and the
356 disturbance is not economically favorable. In this case, both the proposed EMPC and the tracking
357 MPC try to reject the disturbance quickly and drive the system back to a new steady-state operating
358 point. In Fig. 7, the red dotted curve represents the evolution of J_{eco} under the proposed EMPC,
359 and the blue dotted curve represents the evolution of J_{eco} under the tracking MPC. It can be seen
360 that both controllers give similar trajectories.

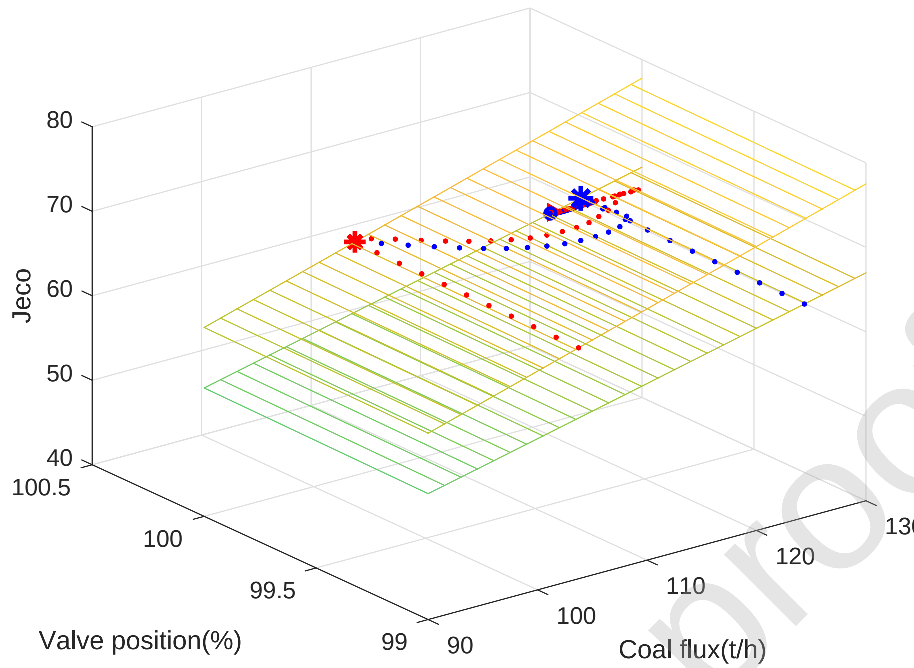

Figure 7: The evolution of economic cost of the system under the proposed EMPC (red dotted line) and the tracking MPC (blue dotted line) in the case of $k_c = 0.8$.

Table 4: E_{eco} of controllers under different k_c with state measurements

E_{eco}	$k_c = 1.2$	$k_c = 1.1$	$k_c = 0.8$	$k_c = 0.9$
EMPC	27357.55 (1.0222)	27254.0 (1.0138)	25936.6 (1.0009)	26570.7 (1.0005)
MPC	26763.38 (1)	26882.2 (1)	25914.2 (1)	26556.9 (1)

The performance index E_{eco} values under a set of k_c values are summarized in Table 4. As can be seen from the table, when k_c increases, the proposed EMPC obtains obvious economic performance enhancement compared with the tracking MPC, and the performance enhancement becomes larger with the increase of k_c. On the other side, when k_c decreases, the proposed EMPC behaves similarly to the tracking MPC and obtains very close economic performance to that of the tracking MPC.

Since disturbances also have a noticeable effect on the state estimation performance of MHE, the economic performance of MHE based EMPC is also studied in this section. Table 5 summarizes

Table 5: E_{eco} of controllers under different k_c with state estimates

E_{eco}	$k_c = 1.2$	$k_c = 1.1$	$k_c = 0.8$	$k_c = 0.9$
EMPC	29450.3 (1.1244)	28261.4 (1.0650)	24605.8 (0.9634)	25840.7 (0.9798)
MPC	26192.5 (1)	26537 (1)	25541.3 (1)	26372.9 (1)

E_{eco} under different k_c values in this case. Compared with Table 4, the economic performance enhancement of the proposed EMPC when $k_c > 1$ is larger than the case when the entire state vector is measured. However, when $k_c < 1$, the economic performance of the EMPC is slightly worse than that of the tracking MPC. This may be due to that when k_c increases, system state estimates are smaller than actual states except x_1, but larger than their original steady-state states. Since this model mismatch is unknown to the controllers, the proposed EMPC will still try to drive the system to the original optimal steady-state by decreasing u_1 and u_2. The decrease in u_1, u_2 and y_1 of the MHE-based EMPC will be smaller than that of the EMPC with state measurements, leading to a smaller decrease in J_{eco}. Therefore, the economic performance loss of the MHE-based EMPC will be less and hence it can obtain better economic performance than the EMPC with state feedback, and vice versa if k_c decreases.

In addition to the coal quality variation, a mismatch in the parameter k_3 is also considered to further evaluate the performance of the proposed EMPC. k_3 is the proportional coefficient between governing stage pressure and the product of throttle valve opening and main steam pressure. In this model, k_3 is considered as a constant; however, it may vary with the turbine operating conditions. Therefore economic performance evaluation of the proposed EMPC and tracking MPC with state measurements are conducted with step increases and decreases in k_3. The results are summarized in Table 6. It shows that when k_3 increases, the proposed EMPC obtains similar economic performance as the tracking MPC, while when k_3 decreases, the proposed EMPC obtains 2.14% more economic performance.

Table 6: E_{eco} of controllers under different k_3 with state measurements

E_{eco}	$k_3 = 0.00913$	$k_3 = 0.00747$
EMPC	27504.5(0.9989)	24527.3 (1.0214)
MPC	27533.8 (1)	24014.0 (1)

6 Conclusions

In this paper, a novel EMPC with zone tracking is proposed for the boiler-turbine coordinated control system to account for system economics during the transients while always prioritizing unit load demand tracking. Extensive simulations were carried out to compare the performance of the proposed EMPC with a conventional two-layer tracking MPC. From the simulations, we see that the proposed EMPC has very close load-tracking capacity compared with the tracking MPC. However, the proposed EMPC provides a more flexible framework due to the integration of a zone tracking objective. It can be used to obtain more economic benefits by tuning the size of the tracking zone. Further, when there is variation in the coal quality, the proposed EMPC can give much improved economic performance especially when only output measurements are available. Overall, the proposed EMPC with zone tracking provides an attractive control alternative to the conventional tacking MPC.

7 Acknowledgements

The research work is supported by the National Nature Science Foundation of China under Grant 51576041 and the China Scholarship Council (CSC).

References

[1] L. Wang, J. J. Li, Y. H. Wang, Q. X. Guan, Research on Coordinated Control System for Boiler-Turbine Units Based on Fractional-Order Control, Advanced Materials Research 732-

733 (2013) 276–279.

[2] R. Garduno-Ramirez, K. Y. Lee, Compensation of control-loop interaction for power plant wide-range operation, Control Engineering Practice 13 (2005) 1475–1487.

[3] Z. Tian, J. Yuan, X. Zhang, L. Kong, J. Wang, Modeling and sliding mode predictive control of the ultra-supercritical boiler-turbine system with uncertainties and input constraints, ISA Transactions 76 (2018) 43–56.

[4] S. Yang, C. Qian, H. Du, A genuine nonlinear approach for controller design of a boilerturbine system, ISA Transactions 51 (2012) 446–453.

[5] W. Tan, F. Fang, L. Tian, C. Fu, J. Liu, Linear control of a boilerturbine unit: Analysis and design, ISA Transactions 47 (2008) 189–197.

[6] H. Liu, S. Li, T. Chai, Intelligent decoupling control of power plant main steam pressure and power output, International Journal of Electrical Power & Energy Systems 25 (2003) 809–819.

[7] S. Li, H. Liu, W. Cai, Y. Soh, Li-Hua Xie, A new coordinated control strategy for boiler-turbine system of coal-fired power plant, IEEE Transactions on Control Systems Technology 13 (2005) 943–954.

[8] M. Sayed, S. M. Gharghory, H. A. Kamal, Gain tuning PI controllers for boiler turbine unit using a new hybrid jump PSO, Journal of Electrical Systems and Information Technology 2 (2015) 99–110.

[9] L. Sun, Q. Hua, D. Li, L. Pan, Y. Xue, K. Y. Lee, Direct energy balance based active disturbance rejection control for coal-fired power plant, ISA Transactions 70 (2017) 486–493.

[10] S. Ghabraei, H. Moradi, G. Vossoughi, Multivariable robust adaptive sliding mode control of

an industrial boilerturbine in the presence of modeling imprecisions and external disturbances: A comparison with type-I servo controller, ISA Transactions 58 (2015) 398–408.

[11] Z. Tian, J. Yuan, L. Xu, X. Zhang, J. Wang, Model-based adaptive sliding mode control of the subcritical boiler-turbine system with uncertainties, ISA Transactions 79 (2018) 161–171.

[12] D. Yu, Z. Xu, Nonlinear Coordinated Control of Drum Boiler Power Unit Based on Feedback Linearization, IEEE Transactions on Energy Conversion 20 (2005) 204–210.

[13] X. Liu, P. Guan, C. W. Chan, Nonlinear Multivariable Power Plant Coordinate Control by Constrained Predictive Scheme, IEEE Transactions on Control Systems Technology 18 (2010) 1116–1125.

[14] T. Yu, K. Chan, J. Tong, B. Zhou, D. Li, Coordinated robust nonlinear boiler-turbine-generator control systems via approximate dynamic feedback linearization, Journal of Process Control 20 (2010) 365–374.

[15] U.-C. Moon, Y. Lee, K. Y. Lee, Practical dynamic matrix control for thermal power plant coordinated control, Control Engineering Practice 71 (2018) 154–163.

[16] G. Wang, W. Yan, S. Chen, X. Zhang, H. Shao, Multi-model Predictive Control of Ultra-supercritical Coal-fired Power Unit, Chinese Journal of Chemical Engineering 22 (2014) 782–787.

[17] F. Zhang, J. Shen, Y. Li, X. Wu, Nonlinear model predictive control of ultra-supercritical once through boiler-turbine unit, in: 2015 Chinese Automation Congress (CAC), IEEE, Wuhan, China, 2015, pp. 2194–2198.

[18] X. Wu, J. Shen, Y. Li, K. Y. Lee, Fuzzy modeling and stable model predictive tracking control of large-scale power plants, Journal of Process Control 24 (2014) 1609–1626.

[19] M. awryczuk, Nonlinear predictive control of a boiler-turbine unit: A state-space approach with successive on-line model linearisation and quadratic optimisation, ISA Transactions 67 (2017) 476–495.

[20] F. Zhang, X. Wu, J. Shen, Extended state observer based fuzzy model predictive control for ultra-supercritical boiler-turbine unit, Applied Thermal Engineering 118 (2017) 90–100.

[21] X. Wu, J. Shen, Y. Li, K. Y. Lee, Hierarchical optimization of boilerturbine unit using fuzzy stable model predictive control, Control Engineering Practice 30 (2014) 112–123.

[22] R. Garduno-Ramirez, K. Lee, Multiobjective optimal power plant operation through coordinate control with pressure set point scheduling, IEEE Transactions on Energy Conversion 16 (2001) 115–122.

[23] Z. Zaharn, R. F. Shi, X. J. Liu, Comparative Study on Multiobjective Power Unit Coordinated Control Problem via Differential Evolution and Particle Swarm Optimization Algorithms, Advanced Materials Research 650 (2013) 470–475.

[24] M. Sayed, S. M. Gharghory, H. A. Kamal, Euclidean distance-based multi-objective particle swarm optimization for optimal power plant set points, Energy Systems 7 (2016) 569–583.

[25] A. Gopalakrishnan, L. T. Biegler, Economic Nonlinear Model Predictive Control for periodic optimal operation of gas pipeline networks, Computers & Chemical Engineering 52 (2013) 90–99.

[26] M. Ellis, P. D. Christofides, Economic model predictive control with time-varying objective function for nonlinear process systems, AIChE Journal 60 (2014) 507–519.

[27] M. Ellis, P. D. Christofides, Economic model predictive control of nonlinear time-delay systems: Closed-loop stability and delay compensation, AIChE Journal 61 (2015) 4152–4165.

[28] J. Zeng, J. Liu, Economic Model Predictive Control of Wastewater Treatment Processes, Industrial & Engineering Chemistry Research 54 (2015) 5710–5721.

[29] T. Broomhead, C. Manzie, P. Hield, R. Shekhar, M. Brear, Economic Model Predictive Control and Applications for Diesel Generators, IEEE Transactions on Control Systems Technology 25 (2017) 388–400.

[30] S. Liu, Y. Mao, J. Liu, Nonlinear model predictive control for zone tracking, IEEE Transactions on Automatic Control (in press).

[31] Y. Mao, S. Liu, J. Nahar, J. Liu, F. Ding, Soil moisture regulation of agro-hydrological systems using zone model predictive control, Computers and Electronics in Agriculture 154 (2018) 239–247.

[32] J. McAllister, Z. Li, J. Liu, U. Simonsmeier, Erythropoietin dose optimization for anemia in chronic kidney disease using recursive zone model predictive control, IEEE Transactions on Control Systems Technology 27 (2019) 1181–1193.

[33] L. Sun, D. Li, K. Y. Lee, Y. Xue, Control-oriented modeling and analysis of direct energy balance in coal-fired boiler-turbine unit, Control Engineering Practice 55 (2016) 38–55.

[34] C. Rao, J. Rawlings, D. Mayne, Constrained state estimation for nonlinear discrete-time systems: stability and moving horizon approximations, IEEE Transactions on Automatic Control 48 (2003) 246–258.

[35] M. Ellis, J. Zhang, J. Liu, P. D. Christofides, Robust moving horizon estimation based output feedback economic model predictive control, Systems & Control Letters 68 (2014) 101–109.

[36] C. V. Rao, J. B. Rawlings, Constrained process monitoring: Moving-horizon approach, AIChE Journal 48 (2002) 97–109.

[37] Joel A. E. Andersson, Joris Gillis, Greg Horn, James B. Rawlings, and Moritz Diehl. CasADi: a software framework for nonlinear optimization and optimal control. *Mathematical Programming Computation*, 11(1):1–36, March 2019.